

000 001 002 003 004 005 ROBUST OPTIMIZATION IN CAUSAL MODELS AND G - 006 CAUSAL NORMALIZING FLOWS 007 008 009

010 **Anonymous authors**
011 Paper under double-blind review
012
013
014
015
016
017
018
019
020

021 ABSTRACT 022

023 In this paper, we show that interventionally robust optimization problems in causal
024 models are continuous under the G -causal Wasserstein distance, but may be dis-
025 continuous under the standard Wasserstein distance. This highlights the impor-
026 tance of using generative models that respect the causal structure when augment-
027 ing data for such tasks. To this end, we propose a new normalizing flow archi-
028 tecture that satisfies a universal approximation property for causal structural mod-
029 els and can be efficiently trained to minimize the G -causal Wasserstein distance.
030 Empirically, we demonstrate that our model outperforms standard (non-causal)
031 generative models in data augmentation for causal regression and mean-variance
032 portfolio optimization in causal factor models.
033

034 1 INTRODUCTION 035

036 Solving optimization problems often requires generative data augmentation (Chen et al., 2024;
037 Zheng et al., 2023), particularly when out-of-sample distributional shifts are expected to be fre-
038 quent and severe, as in the case of financial applications. In such cases, only the most recent data
039 points are representative enough to be used in solving downstream tasks (such as hedging, regression
040 or portfolio selection), resulting in small datasets that require generative data augmentation to avoid
041 overfitting (Bailey et al., 2017). However, when using generative models for data augmentation, it
042 is essential to choose their training loss in a way that is compatible with the downstream tasks, so as
043 to guarantee good and stable performance.

044 It is well-known, for instance, that multi-stage stochastic optimization problems are continuous un-
045 der the *adapted* Wasserstein distance, while they may be discontinuous under the standard Wasser-
046 stein distance (Pflug & Pichler, 2012; 2014; Backhoff-Veraguas et al., 2020). This insight prompted
047 several authors to propose new time-series generative models that attempt to minimize the adapted
048 Wasserstein distance, either partially (Xu et al., 2020) or its one-sided¹ version (Acciaio et al., 2024).

049 In this paper we prove a generalization of this result for causal models. Specifically, we show that
050 causal optimization problems (i.e. problems in which the control variables can depend only on the
051 parents of the state variables in the underlying causal DAG G) are continuous with respect to the
052 G -causal Wasserstein distance (Cheridito & Eckstein, 2025).

053 Furthermore, we prove that solutions to G -causal optimization problems are always interventionally
054 robust. This means that causal optimization can be understood as a way of performing Distribution-
055 ally Robust Optimization (DRO) (Chen et al., 2020; Kuhn et al., 2025) by taking into account the
056 problem’s causal structure.

057 Next, we address the challenge of designing a generative model capable of good approximations un-
058 der the G -causal Wasserstein distance. We radically depart from existing approaches for the adapted
059 Wasserstein distance and propose a novel G -causal normalizing flow model based on invertible neu-
060 ral couplings that respect the causal structure of the data. We prove a universal approximation prop-
061 erty for this model class and that maximum likelihood training indeed leads to distributions that are
062

063 ¹Also known in the literature as the causal Wasserstein distance, because it respects the temporal flow
064 of information in the causal direction (from past to present). This terminology conflicts with the way the
065 term “causal” is used in causal modelling. To avoid misunderstandings we talk of the “ G -causal” Wasserstein
066 distance and refer to the causal Wasserstein distance as the “one-sided” adapted Wasserstein distance.

close to the target distribution in the G -causal Wasserstein distance. Since the standard, adapted and CO-OT Wasserstein distances are all special cases of the G -causal Wasserstein distance, this model family provides optimal generative augmentation models for a vast class of empirical applications.

Contributions. Our main contributions are the following:

- We prove that causal optimization problems (i.e. problems in which optimizers must be functions of the state variables' parents in the causal DAG G) are continuous under the G -causal Wasserstein distance, but may be discontinuous under the standard Wasserstein distance.
- We prove that solutions to G -causal optimization problems are always interventionally robust.
- We introduce G -causal normalizing flows and we prove that they satisfy a universal approximation property for causal structural models under very mild conditions.
- We prove that G -causal normalizing flows minimize the G -causal Wasserstein distance between data and model distribution by simple likelihood maximization.
- We show empirically that G -causal normalizing flows outperform non-causal generative models (such as variational auto-encoders, standard normalizing flows, and nearest-neighbor KDE) when used to perform generative data augmentation in two empirical setups: causal regression and mean-variance portfolio optimization in causal factor models.

2 BACKGROUND

Notation. We denote by $\|\cdot\|$ the Euclidean norm on \mathbb{R}^d and by $L^p(\mu)$ the space $L^p(\mathbb{R}^d, \mathcal{B}(\mathbb{R}^d), \mu)$ equipped with the norm $\|f\|_{L^p(\mu)} := \left(\int_{\mathbb{R}^d} \|f(z)\|^p \mu(dz)\right)^{1/p}$. $\mathcal{P}(\mathbb{R}^d)$ denotes the space of all Borel probability measures on \mathbb{R}^d . $\mathcal{N}(\mu, \Sigma)$ is the multivariate Gaussian distribution with mean μ and covariance matrix Σ , $\mathcal{U}([0, 1]^d)$ is the uniform distribution on the d -dimensional hypercube, I_d denotes the $d \times d$ identity matrix.

We use set-indices to slice vectors, i.e. if $x = (x_1, \dots, x_d) \in \mathbb{R}^d$ and $A \subseteq \{1, \dots, d\}$, then $x_A := (x_i, i \in A) \in \mathbb{R}^{|A|}$. If $\mu \in \mathcal{P}(\mathbb{R}^d)$ and $X = (X_1, \dots, X_d) \sim \mu$, then the regular conditional distribution of X_A given X_B is denoted by $\mu(dx_A | x_B)$, for all $A, B \subseteq \{1, \dots, d\}$ with $A \cap B = \emptyset$.

2.1 STRUCTURAL CAUSAL MODELS

We assume throughout that $G = (V, E)$ is a given directed acyclic graph (DAG) with a finite index set $V = \{1, \dots, d\}$, which we assume, without loss of generality, to be sorted (i.e. $(i, j) \in E$, then $i < j$). If $A \subseteq V$, we denote by $\text{PA}(A) := \{i \in V \setminus A \mid \exists j \in A \mid (i, j) \in E\}$ the set of parents of the vertices in A (notice that $\text{PA}(A) \subseteq V \setminus A$ by definition).

In this paper, we work with structural causal models, as presented in Peters et al. (2017).

Definition 2.1 (Structural Causal Model (SCM)). Given a DAG $G = (V, E)$, a Structural Causal Model (SCM) is a collection of assignments

$$X_i := f_i(X_{\text{PA}(i)}, U_i), \quad \text{for all } i = 1, \dots, d,$$

where the noise variables $(U_i, i = 1, \dots, d)$ are mutually independent.

2.2 G -CAUSAL WASSERSTEIN DISTANCE

Definition 2.2 (G -compatible distribution). A distribution $\mu \in \mathcal{P}(\mathbb{R}^d)$ is said to be G -compatible, and we denote it by $\mu \in \mathcal{P}_G(\mathbb{R}^d)$, if any of the following equivalent conditions holds:

1. there exist a random vector $X = (X_1, \dots, X_d) \sim \mu$ together with measurable functions $f_i : \mathbb{R}^{|\text{PA}(i)|} \times \mathbb{R} \rightarrow \mathbb{R}$, $(i = 1, \dots, n)$, and mutually independent random variables $(U_i, i = 1, \dots, d)$ such that

$$X_i = f_i(X_{\text{PA}(i)}, U_i), \quad \text{for all } i = 1, \dots, d.$$

108 2. For every $X \sim \mu$, one has
 109

$$110 \quad X_i \perp\!\!\!\perp X_{1:i-1} \mid X_{\text{PA}(i)}, \quad \text{for all } i = 2, \dots, d.$$

112 3. The distribution μ admits the following disintegration:

$$113 \quad \mu(dx_1, \dots, dx_d) = \prod_{i=1}^d \mu(dx_i \mid x_{\text{PA}(i)}).$$

117 For a proof of the equivalence of these three conditions, see Cheridito & Eckstein (2025, Remark
 118 3.2).

119 **Definition 2.3** (*G*-bicausal couplings). A coupling $\pi \in \Pi(\mu, \nu)$ between two distributions $\mu, \nu \in$
 120 $\mathcal{P}_G(\mathbb{R}^d)$ is ***G*-causal** if there exist $(X, X') \sim \pi$ such that

$$122 \quad X'_i = g_i(X_i, X_{\text{PA}(i)}, X'_{\text{PA}(i)}, U_i)$$

123 for some measurable mappings $(g_i)_{i=1}^d$ and mutually independent random variables $(U_i)_{i=1}^d$. If also
 124 the distribution of (X', X) is *G*-causal, then we say that π is ***G*-bicausal**. We denote by $\Pi_G^{\text{bc}}(\mu, \nu)$
 125 the set of all *G*-bicausal couplings between μ and ν .

126 **Definition 2.4** (*G*-causal Wasserstein distance). Denote by $\mathcal{P}_{G,1}(\mathbb{R}^d)$ the space of all *G*-compatible
 127 distributions with finite first moments. Then the *G*-causal Wasserstein distance between $\mu, \nu \in$
 128 $\mathcal{P}_{G,1}(\mathbb{R}^d)$ is defined as:

$$130 \quad W_G(\mu, \nu) := \inf_{\pi \in \Pi_G^{\text{bc}}(\mu, \nu)} \int_{\mathbb{R}^d \times \mathbb{R}^d} \|x - x'\| \pi(dx, dx').$$

133 Furthermore, W_G defines a semi-metric on the space $\mathcal{P}_{G,1}(\mathbb{R}^d)$ (Cheridito & Eckstein, 2025, Propo-
 134 sition 4.3).

136 3 ROBUST OPTIMIZATION IN STRUCTURAL CAUSAL MODELS

138 Suppose we are given an SCM $X \sim \mu \in \mathcal{P}_G(\mathbb{R}^d)$ on a DAG $G = (V, E)$ and we want to solve
 139 a stochastic optimization problem in which the state variables X_T are specified by a vertex subset
 140 $T \subseteq V$ (called the *target set*) and the control variables can potentially be all remaining vertices in
 141 the graph, i.e. $X_{V \setminus T}$. To avoid feedback loops between state and control variables, we will need the
 142 following technical assumption.

143 **Assumption 3.1.** The DAG $G = (V, E)$ and the target set $T \subseteq V$ are such that G quotiented by the
 144 partition $\{T\} \cup \{\{i\}, i \in V \setminus T\}$ is a DAG.

145 *Remark 3.2.* Assumption 3.1 is quite mild and is equivalent to asking that if $i, j \in T$, then X_i cannot
 146 be the parent of a parent of X_j . This guarantees that $\text{PA}(T) \cap \text{CH}(T) = \emptyset$, which is nothing but
 147 asking that X_T be part of a valid SCM as a random vector, see Fig. 1 and 2.

148 **Definition 3.3** (*G*-causal function). Given a target set $T \subseteq V$, we say that a function $h : \mathbb{R}^{|V \setminus T|} \rightarrow$
 149 $\mathbb{R}^{|T|}$ is *G*-causal (with respect to T) if h depends only on the parents of X_T , i.e. $h(x) = h(x_{\text{PA}(T)})$,
 150 for all $x \in \mathbb{R}^{|V \setminus T|}$.

152 **Definition 3.4** (*G*-causal optimization problem). Let $G = (V, E)$ be a sorted DAG, $X \sim \mu \in$
 153 $\mathcal{P}_G(\mathbb{R}^d)$ and let $T \subseteq V$ be a target set. If $Q : \mathbb{R}^{|T|} \times \mathbb{R}^{|V \setminus T|} \rightarrow \mathbb{R}$ is a function to be optimized, then
 154 a *G*-causal optimization problem (with respect to T) is an optimization problem of the following
 155 form:

$$156 \quad \min_{\substack{h: \mathbb{R}^{|V \setminus T|} \rightarrow \mathbb{R}^{|T|} \\ h \text{ is } G\text{-causal}}} \mathbb{E}^\mu [Q(X_T, h(X_{V \setminus T}))]. \quad (1)$$

158 Any minimizer of (1) is called a *G*-causal optimizer.

160 The following result shows that *G*-causal optimizers are always interventionally robust. This un-
 161 derscores the desirability of *G*-causal optimizers when we expect the data distribution to undergo
 162 distributional shifts due to interventions between training and testing time.

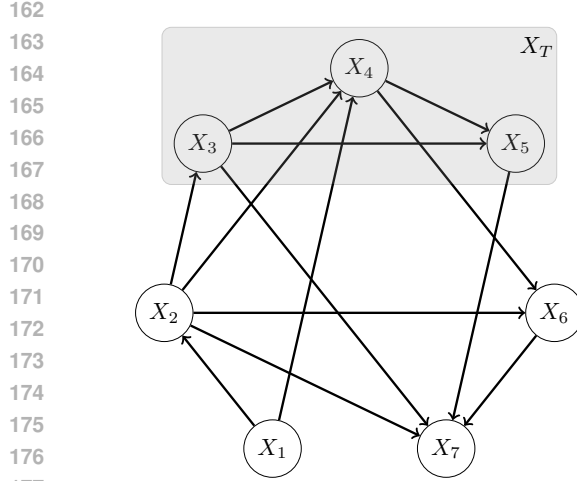


Figure 1: DAG G before quotienting (target set T highlighted).

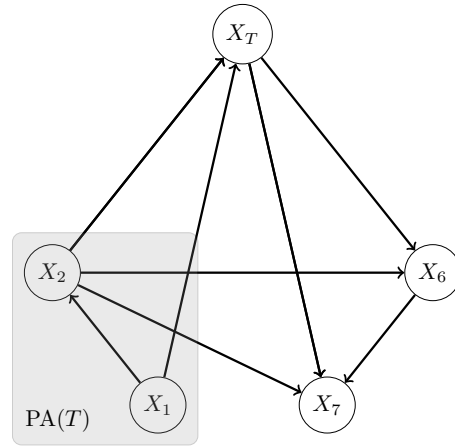


Figure 2: DAG G after quotienting (vertex set $PA(T)$ highlighted).

Theorem 3.5 (Robustness of G -causal optimizers). *Let h^* be a solution of the problem in Eq. (1). Then:*

$$h^* \in \arg \min_{h: \mathbb{R}^{|V \setminus T|} \rightarrow \mathbb{R}^{|T|}} \sup_{\nu \in \mathcal{I}(\mu)} \mathbb{E}^\nu [Q(X_T, h(X_{V \setminus T}))],$$

where

$\mathcal{I}(\mu) := \{\nu \in \mathcal{P}(\mathbb{R}^d) \mid \nu(dx_T | x_{PA(T)}) = \mu(dx_T | x_{PA(T)}) \text{ and } \text{supp}(\nu(dx_{PA(T)})) \subseteq \text{supp}(\mu(dx_{PA(T)}))\}$
is the set of all interventional distributions that leave the causal mechanism of X_T unchanged.

Proof. It's enough to show that for any $h: \mathbb{R}^{|V \setminus T|} \rightarrow \mathbb{R}^{|T|}$ and any $\nu \in \mathcal{I}(\mu)$, there exists a $\nu' \in \mathcal{I}(\mu)$ such that $\mathbb{E}^{\nu'} [Q(X_T, h(X_{V \setminus T}))] \geq \mathbb{E}^\nu [Q(X_T, h^*(X_{PA(T)}))]$.

Given $\nu \in \mathcal{I}(\mu)$, define $\nu'(dx) := \nu(dx_{V \setminus (T \cup PA(T))}) \nu(dx_{PA(T)}, dx_T)$. Then:

$$\begin{aligned} \mathbb{E}^{\nu'} [Q(X_T, h(X_{V \setminus T}))] &= \int \nu(dx_{V \setminus (T \cup PA(T))}) \int \nu(dx_{PA(T)}, dx_T) Q(x_T, h(x_{V \setminus T})) \\ &= \int \nu(dx_{V \setminus (T \cup PA(T))}) \int \nu(x_{PA(T)}) \int \mu(dx_T | x_{PA(T)}) Q(x_T, h(x_{V \setminus T})) \\ &\geq \int \nu(dx_{V \setminus (T \cup PA(T))}) \int \nu(x_{PA(T)}) \int \mu(dx_T | x_{PA(T)}) Q(x_T, h^*(x_{PA(T)})) \\ &= \mathbb{E}^\nu [Q(X_T, h^*(X_{PA(T)}))] \end{aligned}$$

where the second equality follows from $\nu \in \mathcal{I}(\mu)$ and the inequality follows from Eq. (1), Lemma A.1, and $\text{supp}(\nu(dx_{PA(Y)})) \subseteq \text{supp}(\mu(dx_{PA(Y)}))$. \square

Remark 3.6. The theorem above is a generalization of (Rojas-Carulla et al., 2018, Theorem 4), which covered the mean squared loss only. We explicitly added the assumption $\text{supp}(\nu(dx_{PA(Y)})) \subseteq \text{supp}(\mu(dx_{PA(Y)}))$, for all $\nu \in \mathcal{I}(\mu)$, which is needed also for their theorem to hold.

The next theorem shows that the value functionals of G -causal optimization problems are continuous with respect to the G -causal Wasserstein distance, while they may fail to be continuous with respect to the standard Wasserstein distance (as we show in Example 3.8 below). This proves that the G -causal Wasserstein distance is the right distance to control errors in causal optimization problems and, in particular, interventionally robust optimization problems.

Theorem 3.7 (Continuity of G -causal optimization problems). *Let $G = (V, E)$ be a sorted DAG, $X \sim \mu \in \mathcal{P}_G(\mathbb{R}^d)$ and let $T \subseteq V$ be a target set, such that Assumption 3.1 holds. If $Q: \mathbb{R}^{|T|} \times$*

216 $\mathbb{R}^{|V \setminus T|} \rightarrow \overline{\mathbb{R}}$ is such that $x \mapsto Q(x, h)$ is locally L -Lipschitz (uniformly in h) and $h \mapsto Q(x, h)$ is
 217 convex, then the value functional

$$219 \quad \mu \mapsto \mathcal{V}(\mu) := \min_{\substack{h: \mathbb{R}^{|V \setminus T|} \rightarrow \mathbb{R}^{|T|} \\ h \text{ is } G\text{-causal}}} \mathbb{E}^\mu [Q(X_T, h(X_{V \setminus T}))]$$

221 is continuous with respect to the G -causal Wasserstein distance.

223 *Proof.* See proof in Appendix B.1. □

225 **Example 3.8.** Define $\mu_\varepsilon \in \mathcal{P}_G(\mathbb{R}^2)$ as the following SCM:

$$227 \quad \begin{cases} Y := \text{sgn}(X), \\ X := \varepsilon \cdot U, \end{cases} \quad \text{where } U \sim \text{Ra}(1/2),$$

229 where $\text{Ra}(p)$ denoted the Rademacher distribution $p\delta_1 + (1-p)\delta_{-1}$, and consider the following
 230 G -causal regression problem:

$$232 \quad \mathcal{V}(\mu) = \inf_{\substack{h: \mathbb{R} \rightarrow \mathbb{R} \\ h \text{ } G\text{-causal}}} \mathbb{E}^\mu [(Y - h(X))^2].$$

234 Then as $\varepsilon \rightarrow 0$ we have that $\mu_\varepsilon = \frac{1}{2}\delta_{(\varepsilon, 1)} + \frac{1}{2}\delta_{(-\varepsilon, -1)}$ converges to $\mu := \frac{1}{2}\delta_{(0, 1)} + \frac{1}{2}\delta_{(0, -1)} =$
 235 $\delta_0 \otimes \text{Ra}(1/2)$ under the standard Wasserstein distance, but $\lim_{\varepsilon \rightarrow 0} \mathcal{V}(\mu_\varepsilon) = 0 \neq 1 = \mathcal{V}(\mu)$.

238 4 PROPOSED METHOD: G -CAUSAL NORMALIZING FLOWS

240 Theorem 3.7 and Example 3.8 imply that generative augmentation models that are not trained under
 241 the G -causal Wasserstein distance may lead to optimizers that severely underperform on G -causal
 242 downstream tasks. To solve this issue, we propose a novel normalizing flow architecture capable of
 243 minimizing the G -causal Wasserstein distance from any data distribution $\mu \in \mathcal{P}_G(\mathbb{R}^d)$. Since the
 244 standard, adapted and CO-OT Wasserstein distances are all special cases of the G -causal Wasserstein
 245 distance, this model family provides optimal generative augmentation models for a vast class of
 246 empirical applications.

247 A G -causal normalizing flow $\hat{T} = \hat{T}^{(d)} \circ \dots \circ \hat{T}^{(1)}$ is a composition of d neural coupling flows
 248 $\hat{T}^{(k)} : \mathbb{R}^d \rightarrow \mathbb{R}^d$ of the following form:

$$250 \quad \hat{T}_i^{(k)}(x) = \begin{cases} g(x_i; \theta(x_{\text{PA}(i)})) & \text{if } i = k \\ \text{id} & \text{if } i \neq k \end{cases} \quad (2)$$

252 where $g : \mathbb{R} \times \Theta(n) \rightarrow \mathbb{R}$ is a shallow MLP of the form:

$$254 \quad g(x, \theta) = \sum_{i=1}^n w_i^{(2)} \rho(w_i^{(1)} x + b_i^{(1)}) + b^{(2)} \quad (3)$$

257 with parameters $\theta := (w^{(1)}, b^{(1)}, w^{(2)}, b^{(2)}) \in \Theta(n) := \mathbb{R}_{>0}^n \times \mathbb{R}^n \times \mathbb{R}_{>0}^n \times \mathbb{R}$ and custom activation
 258 function²:

$$260 \quad \rho(x) = \frac{1}{2} \text{LeakyReLU}_{\alpha-1}(1+x) - \frac{1}{2} \text{LeakyReLU}_{\alpha-1}(1-x), \quad \alpha \in (0, 1). \quad (4)$$

262 We denote by $\text{IncrMLP}(n)$ the class of all MLPs with n hidden neurons and parameter space $\Theta(n)$.
 263 It is easy to see that $\text{IncrMLP}(n)$ contains only continuous, piecewise linear, strictly increasing (and,
 264 therefore, *invertible*) functions, thanks to the choice of activation function³ and parameter space. The
 265 inverse of g and its derivative can be computed efficiently, which allows the coupling flow in Eq. (2)
 266 to be easily implemented in a normalizing flow model (see code in the supplementary material).

267 ²Recall that the LeakyReLU activation function is defined as $\text{LeakyReLU}_\alpha(x) := x\mathbb{1}_{\{x \geq 0\}} + \alpha x\mathbb{1}_{\{x < 0\}}$.

268 ³One cannot just take $\rho(x) = \text{ReLU}(x)$, because g could fail to be strictly increasing, nor $\rho(x) =$
 269 $\text{LeakyReLU}_\alpha(x)$, because then g would be constrained to be convex, which harms model capacity.

In Eq. (2) we specify the parameters of g in terms of a function $\theta(x_{\text{PA}(i)})$, which we take to be an MLP⁴. The particular choice of MLP class does not matter, as long as the assumptions of (Leshno et al., 1993, Theorem 1) are satisfied⁵ and we denote by MLP any such class. Since the outputs of $\theta(\cdot) \in \text{MLP}$ are used as parameters for another MLP, $g(\cdot)$, it is common to say that $\theta(\cdot)$ is a *hypernetwork* (Chauhan et al., 2024). Therefore we say that the coupling flow in Eq. (2) is a hypercoupling flow and we denote by $\text{HyperCpl}(n, \theta(\cdot))$ the class of hypercoupling flows with $g(\cdot) \in \text{IncrMLP}(n)$ and parameter hypernetwork $\theta(\cdot) \in \text{MLP}$.

Since each hypercoupling flow in a G -causal normalizing flow acts only on a subset of the input coordinates it effectively functions as a scale in a multi-scale architecture, thus reducing the computational burden by exploiting our a priori knowledge of the causal DAG G .

Remark 4.1. We emphasize that the DAG G is an *input* of our model, not an output. We assume, therefore, that the modeler has estimated the causal skeleton G , using any of the available methods for causal discovery Nogueira et al. (2022); Zanga et al. (2022). On the other hand, we do not require any knowledge of the functional form of the causal mechanisms, which our model will learn directly from data.

Next, we turn to the task of proving that G -causal normalizing flows are universal approximators for structural causal models.

Definition 4.2 (G -compatible transformation.). Let G be a sorted DAG. A map $T : \mathbb{R}^d \rightarrow \mathbb{R}^d$ is a G -compatible transformation if each coordinate $T_i(x)$ is a function of $(x_i, x_{\text{PA}(i)})$, for all $i = 1, \dots, d$. Furthermore, a G -compatible transformation T is called (strictly) increasing if each coordinate T_i is (strictly) increasing in x_i .

Theorem 4.3. Let $\mu \in \mathcal{P}_G(\mathbb{R}^d)$ be an absolutely continuous distribution. Then there exists a G -compatible, strictly increasing transformation $T : \mathbb{R}^d \rightarrow \mathbb{R}^d$, such that $T_{\#}\mathcal{U}([0, 1]^d) = \mu$.

Furthermore, T is of the form $T := T^{(d)} \circ \dots \circ T^{(1)}$, where each $T^{(k)} : \mathbb{R}^d \rightarrow \mathbb{R}^d$ is defined as:

$$T_i^{(k)}(x) = \begin{cases} F_i^{-1}(x_i \mid x_{\text{PA}(i)}) & i = k, \\ \text{id} & i \neq k. \end{cases} \quad (k = 1, \dots, d)$$

where F_i^{-1} is the (conditional) quantile function of the random variable $X_i \sim \mu(dx_i)$ given its parents $X_{\text{PA}(i)} \sim \mu(dx_{\text{PA}(i)})$.

Proof. It is easy to check that T , as defined, is indeed a G -compatible, increasing transformation. The absolute continuity of μ implies that all conditional distributions admit a density (Jacod & Protter, 2004, Theorem 12.2), therefore a continuous cdf and a strictly monotone quantile function (McNeil et al., 2015, Proposition A.3 (ii)).

Next, we show that $T_{\#}\mathcal{U}([0, 1]^d) = \mu$. By Definition 2.2 we know that there exists $X \sim \mu$ and measurable functions f_i such that $X_i = f_i(X_{\text{PA}(i)}, U_i)$ where $U = (U_1, \dots, U_d)$ is a random vector of mutually independent random variables. Without loss of generality, we can take $U \sim \mathcal{U}([0, 1]^d)$ and set $X_i = F_i^{-1}(U_i \mid X_{\text{PA}(i)})$ (McNeil et al., 2015, Proposition A.6). \square

Theorem 4.4 (Universal Approximation Property (UAP) for G -causal normalizing flows). Let $\mu \in \mathcal{P}_{G,1}(\mathbb{R}^d)$ be an absolutely continuous distribution with compact support and assume that the conditional cdfs $(x_k, x_{\text{PA}(k)}) \mapsto F_k(x_k \mid x_{\text{PA}(k)})$ belong to $C^1(\mathbb{R} \times \mathbb{R}^{|\text{PA}(k)|})$, for all $k = 1, \dots, d$.

Then G -causal normalizing flows with base distribution $\mathcal{U}([0, 1]^d)$ are dense in the semi-metric space $(\mathcal{P}_{G,1}(\mathbb{R}^d), W_G)$, i.e. for every $\varepsilon > 0$, there exists a G -causal normalizing flow \hat{T} such that

$$W_G(\mu, \hat{T}_{\#}\mathcal{U}([0, 1]^d)) \leq \varepsilon.$$

Proof. See proof in Appendix B.2. \square

⁴In practice, we enforce $\theta(x_{\text{PA}(i)}) \in \Theta(n)$ by constraining its outputs corresponding to the weights $w^{(1)}$ and $w^{(2)}$ to be strictly positive, either by using a ReLU activation function or by taking their absolute value.

⁵The activation function must be non-polynomial and locally essentially bounded on \mathbb{R} . All commonly used activation functions (including ReLU) satisfy this.

Remark 4.5. The theorem holds for base distributions other than $\mathcal{U}([0, 1]^d)$. In fact any absolutely continuous distribution on \mathbb{R}^d with mutually independent coordinates (such as the standard multivariate Gaussian $\mathcal{N}(0, I_d)$) would work, provided we add a non-trainable layer between the base distribution and the first flow that maps \mathbb{R}^d into the base distribution's quantiles (for $\mathcal{N}(0, I_d)$, such a map is just $\Phi^{\otimes d}$, where Φ is the standard Gaussian cdf).

In practice G -causal normalizing flows are trained using likelihood maximization (or, equivalently, KL minimization), so it is important to make sure that minimizing this loss guarantees that the G -causal Wasserstein distance between data and model distribution is also minimized. The following result proves exactly this and is a generalization of Acciaio et al. (2024, Lemma 2.3) and Eckstein & Pammer (2024, Lemma 3.5), which established an analogous claim for the adapted Wasserstein distance.

Theorem 4.6 (W_G training via KL minimization). *Let $\mu, \nu \in \mathcal{P}_G(K)$ for some compact $K \subseteq \mathbb{R}^d$. Then:*

$$W_G(\mu, \nu) \leq C \sqrt{\frac{1}{2} \mathcal{D}_{KL}(\mu \mid \nu)},$$

for a constant $C > 0$.

Proof. See proof in Appendix B.3.

5 NUMERICAL EXPERIMENTS

5.1 CAUSAL REGRESSION

We study a multivariate causal regression problem of the form:

$$\min_{\substack{h: \mathbb{R}^{|V \setminus T|} \rightarrow \mathbb{R}^{|T|} \\ h \text{ is } G\text{-causal}}} \mathbb{E}^\mu \left[(X_T - h(X_{V \setminus T}))^2 \right], \quad (6)$$

where $\mu \in \mathcal{P}_G(\mathbb{R}^d)$ is a randomly generated linear Gaussian SCM (Peters et al., 2017, Section 7.1.3) with coefficients uniformly sampled in $(-1, 1)$ and homoscedastic noise with unit variance. The sorted DAG G is obtained by randomly sampling an Erdos-Renyi graph on d vertices with edge probability p and eliminating all edges (i, j) with $i > j$.

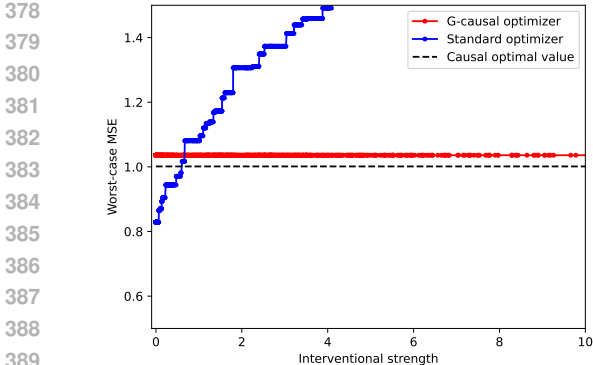
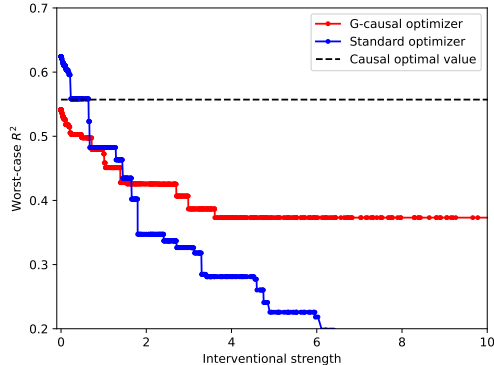
According to Theorem 3.5, any solution to problem (6) is interventionally robust. In order to showcase this robustness property of the G -causal regressor, we compare its performance with that of a standard (i.e. non-causal) regressor when tested out-of-sample on a large number of random soft⁶ interventions. Each intervention is obtained by randomly sampling a node $i \in V \setminus T$ and substituting its causal mechanism, $f(X_{\text{PA}(i)}, U_i)$, with a new one, $\tilde{f}(X_{\text{PA}(i)}, U_i)$. We consider only linear interventions and quantify their interventional strength by computing the following L^1 -norm:

$$\int \int |f(x_{\text{PA}(i)}, u) - \tilde{f}(x_{\text{PA}(i)}, u)| \mu(dx_{\text{PA}(i)}) \lambda(du),$$

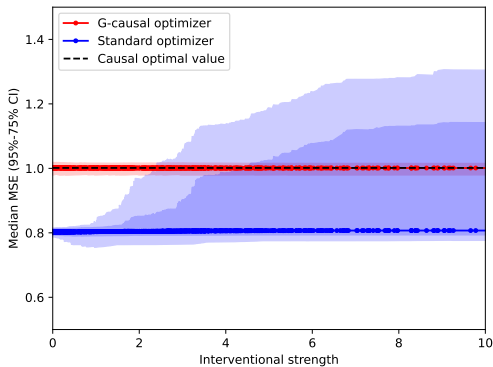
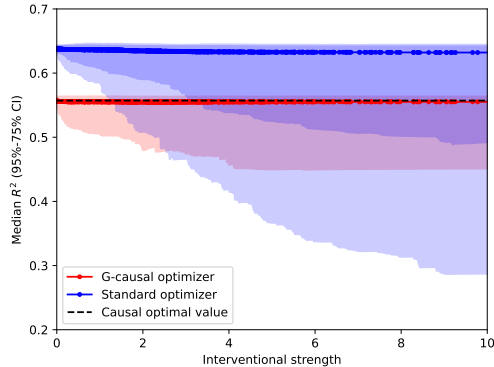
where μ is the original distribution (before intervention) and λ is the noise distribution. Interventional strength, therefore, quantifies the out-of-sample variation of the regressor's inputs under the intervention.

We implement a multivariate regression with $d = 10$, $p = 0.5$ and $T = \{5, 6\}$. We report in Fig. 7 and Fig. 8 the worst-case performance of a G -causal regressor and of a non-causal regressor (in terms of MSE and R^2 , respectively) as a function of the interventional strength. At small interventional strengths the non-causal regressor benefits from the information contained in non-parent nodes (which are not available as inputs to the G -causal optimizer). These non-parent nodes may belong to the Markov blanket of the target nodes in G and therefore be statistically informative, but their usefulness crucially depends on the stability of their causal mechanisms. As the interventional strength is increased the worst-case performance of the non-causal regressor rapidly deteriorates, while that of the G -causal regressor remains stable, as shown in the figures.

⁶A soft intervention at a node $i \in V$ leaves its parents and noise distribution unaltered, but changes the functional form of its causal mechanism.

391
392 Figure 3: Worst-case MSE vs interventional
393 strength.
394391
392 Figure 4: Worst-case R^2 vs interventional
393 strength.
394

In Fig. 5 and Fig. 6 we deepen the comparison by plotting the distribution of the performance metrics (MSE and R^2 , respectively) for both estimators. Notice how interventions deteriorate the performance of the non-causal regressor starting from the least favorable quantiles, while the entire distribution of the performance metrics of the G -causal remains stable. These figures also show that the median performance of the causal regressor is, after all, not strongly affected by the linear random interventions we consider. In this sense, non-causal optimizers can still be approximately optimal in applications where distributional shifts are expected to be mild.

415
416 Figure 5: Median and (75%-95%) CI of MSE
417 vs interventional strength.
418415
416 Figure 6: Median and (75%-95%) CI of R^2 vs
417 interventional strength.
418

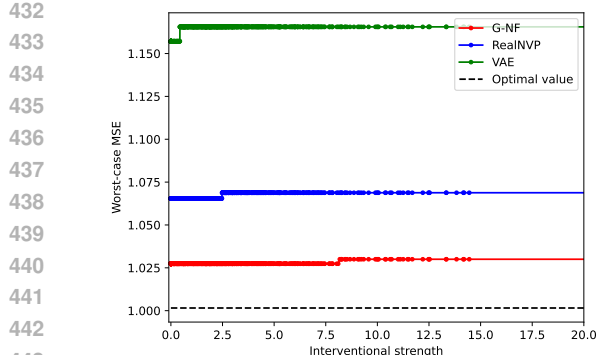
Finally, we investigate the performance of our G -causal normalizing flow model when used for generative data augmentation. We therefore train several augmentation models (both non-causal and G -causal) on a training set of $n = 10000$ samples from μ . We then use them to generate of synthetic training set of $n = 10000$ samples and we train a causal optimizer on it.

As shown in Fig. 7 and Fig. 8, causal optimizers trained using non-causal augmentation models (e.g. RealNVP and VAE) are indeed robust under interventions, but their worst-case metrics are significantly worse than when causal augmentation is used. This is an empirical validation of the fact that the loss used for training the augmentation model plays a crucial role in downstream performance.

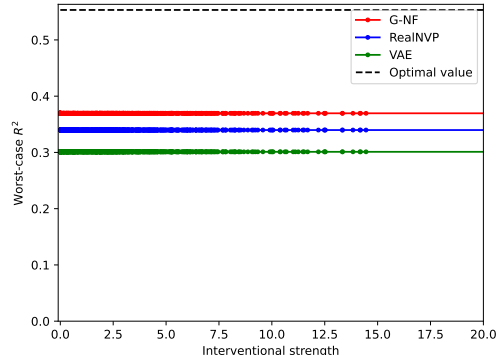
5.2 CONDITIONAL MEAN-VARIANCE PORTFOLIO OPTIMIZATION

We look at the following conditional mean-variance portfolio optimization problem:

$$\mathcal{V}(\mu) = \inf_{\substack{h: \mathbb{R}^{|V \setminus T|} \rightarrow \mathbb{R}^{|T|} \\ h \text{ is } G\text{-causal}}} \left\{ -\mathbb{E}^\mu [\langle X_T, h(X_{V \setminus T}) \rangle] + \frac{\gamma}{2} \text{Var}^\mu (\langle X_T, h(X_{V \setminus T}) \rangle) \right\},$$



445 Figure 7: Worst-case MSE after generative
446 data augmentation vs interventional strength.
447

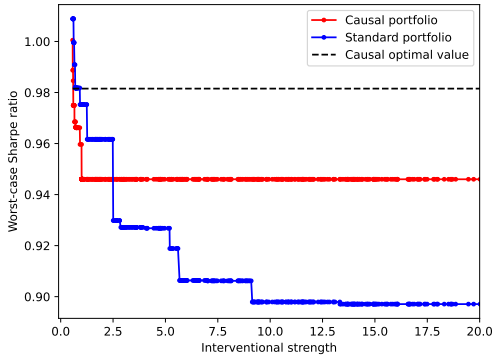


445 Figure 8: Worst-case R^2 after generative data
446 augmentation vs interventional strength.
447

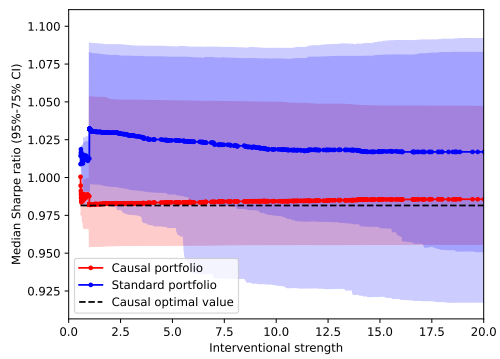
449 where $X \sim \mu \in \mathcal{P}_G(\mathbb{R}^d)$ is a linear Gaussian SCM, with bipartite DAG G with partition $\{T, V \setminus T\}$
450 and random uniform coefficients in $(-1, 1)$, and γ is a given risk aversion parameter. The target
451 variables X_T represent stock returns, while $X_{V \setminus T}$ are market factors or trading signals. We present
452 the results for a high-dimensional example with $|T| = 100$ stocks and $|V \setminus T| = 20$ factors.

453 We sample random linear interventions exactly as done in the case of causal regression and study
454 empirically the robustness of the G -causal portfolio in terms of its Sharpe ratio as the interventional
455 strength increases.

456 Fig. 9 and Fig. 10 show that the Sharpe ratio of the G -causal portfolio is indeed robust to a wide
457 range of interventions, while the performance of non-causal portfolios deteriorates rapidly, starting
458 from the least favorable quantiles.



473 Figure 9: Worst-case Sharpe ratio vs interven-
474 tional strength
475



473 Figure 10: Median and (75%-95%) CI of
474 Sharpe ratio vs interventional strength
475

476 **Reproducibility statement.** All results can be reproduced using the source code provided in the
477 Supplementary Materials. Demo notebooks of the numerical experiments will be made available in
478 a paper-related GitHub repository upon publication.

481 REFERENCES

482
483 Beatrice Acciaio, Stephan Eckstein, and Songyan Hou. Time-Causal VAE: Robust Financial Time
484 Series Generator. *arXiv preprint arXiv:2411.02947*, 2024.
485
Jean-Pierre Aubin and Hélène Frankowska. Set-Valued Analysis, 2009.

486 Julio Backhoff-Veraguas, Daniel Bartl, Mathias Beiglböck, and Manu Eder. Adapted wasserstein
 487 distances and stability in mathematical finance. *Finance and Stochastics*, 24(3):601–632, 2020.
 488

489 David Bailey, Jonathan Borwein, Marcos Lopez de Prado, and Qiji Jim Zhu. The probability of
 490 backtest overfitting. *The Journal of Computational Finance*, 20(4):39–69, 2017.
 491

492 Vladimir I Bogachev. *Measure theory*. Springer, 2007.
 493

493 Vinod Kumar Chauhan, Jiandong Zhou, Ping Lu, Soheila Molaei, and David A Clifton. A brief
 494 review of hypernetworks in deep learning. *Artificial Intelligence Review*, 57(9):250, 2024.
 495

495 Ruidi Chen, Ioannis Ch Paschalidis, et al. Distributionally robust learning. *Foundations and Trends®*
 496 in Optimization, 4(1-2):1–243, 2020.
 497

498 Yunhao Chen, Zihui Yan, and Yunjie Zhu. A comprehensive survey for generative data augmentation.
 499 *Neurocomputing*, 600:128167, 2024.
 500

500 Patrick Cheridito and Stephan Eckstein. Optimal transport and Wasserstein distances for causal
 501 models. *Bernoulli*, 31(2):1351–1376, 2025.
 502

503 Stephan Eckstein and Marcel Nutz. Quantitative stability of regularized optimal transport and con-
 504 vergence of sinkhorn’s algorithm. *SIAM Journal on Mathematical Analysis*, 54(6):5922–5948,
 505 2022.
 506

506 Stephan Eckstein and Gudmund Pammer. Computational methods for adapted optimal transport.
 507 *The Annals of Applied Probability*, 34(1A):675–713, 2024.
 508

509 Gerald B. Folland. *Real Analysis: Modern Techniques and their Applications*. John Wiley & Sons,
 510 1999.
 511

511 Jean Jacod and Philip Protter. *Probability Essentials*. Springer Science & Business Media, 2004.
 512

513 Daniel Kuhn, Soroosh Shafiee, and Wolfram Wiesemann. Distributionally robust optimization. *Acta
 514 Numerica*, 34:579–804, 2025.
 515

515 Moshe Leshno, Vladimir Ya Lin, Allan Pinkus, and Shimon Schocken. Multilayer feedforward net-
 516 works with a nonpolynomial activation function can approximate any function. *Neural networks*,
 517 6(6):861–867, 1993.
 518

519 Alexander J McNeil, Rüdiger Frey, and Paul Embrechts. *Quantitative Risk Management: Concepts,
 520 Techniques and Tools (Revised Edition)*. Princeton university press, 2015.
 521

522 Ana Rita Nogueira, Andrea Pugnana, Salvatore Ruggieri, Dino Pedreschi, and João Gama. Methods
 523 and tools for causal discovery and causal inference. *Wiley interdisciplinary reviews: data mining
 and knowledge discovery*, 12(2):e1449, 2022.
 524

525 Jonas Peters, Dominik Janzing, and Bernhard Schölkopf. *Elements of Causal Inference: Founda-
 526 tions and Learning Algorithms*. The MIT press, 2017.
 527

527 Georg Ch Pflug and Alois Pichler. A distance for multistage stochastic optimization models. *SIAM
 528 Journal on Optimization*, 22(1):1–23, 2012.
 529

530 Georg Ch Pflug and Alois Pichler. *Multistage Stochastic Optimization*, volume 1104. Springer,
 531 2014.
 532

532 R. Tyrrell Rockafellar and Roger J. B. Wets. *Variational Analysis*. Springer, 1998.
 533

534 Mateo Rojas-Carulla, Bernhard Schölkopf, Richard Turner, and Jonas Peters. Invariant Models for
 535 Causal Transfer Learning. *Journal of Machine Learning Research*, 19(36):1–34, 2018.
 536

536 Larry Schumaker. *Spline Functions: Basic Theory*. Cambridge University Press, 2007.
 537

538 Tianlin Xu, Li Kevin Wenliang, Michael Munn, and Beatrice Acciaio. Cot-gan: Generating sequen-
 539 tial data via causal optimal transport. *Advances in neural information processing systems*, 33:
 8798–8809, 2020.

540 Alessio Zanga, Elif Ozkirimli, and Fabio Stella. A survey on causal discovery: theory and practice.
 541 *International Journal of Approximate Reasoning*, 151:101–129, 2022.
 542

543 Chenyu Zheng, Guoqiang Wu, and Chongxuan Li. Toward understanding generative data augmentation.
 544 *Advances in neural information processing systems*, 36:54046–54060, 2023.
 545

546 **A AUXILIARY RESULTS**

549 **Lemma A.1** (Interchangeability principle). *Let $(\Omega, \mathcal{F}, \mathbb{P})$ be a probability space and let $f : \Omega \times \mathbb{R}^d \rightarrow \overline{\mathbb{R}}$ be an \mathcal{F} -measurable normal integrand. Then:*

551
$$\int \min_{x \in \mathbb{R}^d} f(\omega, x) \mathbb{P}(d\omega) = \min_{X \in m\mathcal{F}} \int f(\omega, X(\omega)) \mathbb{P}(d\omega),$$

 552
 553

554 provided that the right-hand side is not ∞ .

555 Furthermore, if both sides are not $-\infty$, then:

557
$$X^* \in \arg \min_{X \in m\mathcal{F}} \int f(\omega, X(\omega)) \mathbb{P}(d\omega) \iff X^*(\omega) \in \arg \min_{x \in \mathbb{R}^d} f(\omega, x), \text{ } (\mu\text{-almost surely})$$

 558
 559

560 *Proof.* See Rockafellar & Wets (1998, Theorem 14.60). \square

561 **Lemma A.2** (Composition lemma). *Let $(\mathcal{X}, \|\cdot\|)$ be a Banach space with its Borel σ -algebra and let
 562 $\mu^{(0)}, \dots, \mu^{(d)}$ be measures defined on it. Given measurable maps $\hat{T}^{(k)} : \mathcal{X} \rightarrow \mathcal{X}$ and $T^{(k)} : \mathcal{X} \rightarrow \mathcal{X}$
 563 such that $T^{(k)} \# \mu^{(k-1)} = \mu^{(k)}$ (for $k = 1, \dots, d$), if the following two conditions hold:*

564 *i) $\hat{T}^{(k)}$ is L_k -Lipschitz,*

565 *ii) $\|T^{(k)} - \hat{T}^{(k)}\|_{L^p(\mu^{(k-1)})} \leq \varepsilon_k$,*

566 *then:*

567
$$\|T^{(d)} \circ \dots \circ T^{(1)} - \hat{T}^{(d)} \circ \dots \circ \hat{T}^{(1)}\|_{L^p(\lambda)} \leq \sum_{k=1}^d \varepsilon_k \prod_{j=k+1}^d L_j,$$

 568
 569

570 with the convention that $\prod_{j \in \emptyset} L_j := 1$.

571 *Proof.* The claim follows by induction. It is obviously true for $d = 1$. Assume that it holds for $d - 1$,
 572 then for d :

573
$$\begin{aligned} & \|T^{(d)} \circ \dots \circ T^{(1)} - \hat{T}^{(d)} \circ \dots \circ \hat{T}^{(1)}\|_{L^p(\mu^{(0)})} \\ & \leq \|T^{(d)} \circ T^{(d-1)} \circ \dots \circ T^{(1)} - \hat{T}^{(d)} \circ T^{(d-1)} \circ \dots \circ T^{(1)}\|_{L^p(\mu^{(0)})} + \\ & \quad \|\hat{T}^{(d)} \circ T^{(d-1)} \circ \dots \circ T^{(1)} - \hat{T}^{(d)} \circ \hat{T}^{(d-1)} \circ \dots \circ \hat{T}^{(1)}\|_{L^p(\mu^{(0)})} \\ & \leq \|T^{(d)} - \hat{T}^{(d)}\|_{L^p(\mu^{(d-1)})} + L_d \|T^{(d-1)} \circ \dots \circ T^{(1)} - \hat{T}^{(d-1)} \circ \dots \circ \hat{T}^{(1)}\|_{L^p(\mu^{(0)})} \end{aligned}$$

 574
$$\text{(Change of variable + Lipschitz)}$$

 575

576
$$\begin{aligned} & \leq \varepsilon_d + L_d \cdot \sum_{k=1}^{d-1} \varepsilon_k \prod_{j=k+1}^{d-1} L_j \quad \text{(claim holds of } d-1) \\ & = \sum_{k=1}^d \varepsilon_k \prod_{j=k+1}^d L_j \end{aligned}$$

 577
 578

579 **Lemma A.3.** *Let $g \in \text{IncrMLP}(n)$ with parameter space $\Theta(n)$. Then the map $\theta \mapsto g(\cdot; \theta)$ from
 580 $\Theta(n)$ to $L^1([0, 1])$ is continuous.*

594 *Proof.* It is a direct application of Lebesgue's dominated convergence theorem (Bogachev, 2007,
595 Theorem 2.8.1), so we just verify that the assumptions of the theorem hold. Let $\theta_k \rightarrow \theta \in \Theta$ be
596 any convergent sequence. Since $\theta \mapsto g(u; \theta)$ is continuous, we have that $g(u; \theta_k) \rightarrow g(u; \theta)$ for all
597 $u \in [0, 1]$. Furthermore, the functions $g(\cdot; \theta_k)$ are uniformly bounded:

$$\begin{aligned} 599 \quad \sup_{k \in \mathbb{N}} |g(u; \theta_k)| &\leq \sup_{k \in \mathbb{N}} \sup_{u \in [0, 1]} |g(u; \theta_k)| \\ 600 \quad &\leq \sup_{k \in \mathbb{N}} \max\{|g(0; \theta_k)|, |g(1; \theta_k)|\} \quad (u \mapsto g(u; \theta) \text{ is increasing}) \\ 601 \quad &\leq \sup_{\theta \in K} \max\{|g(0; \theta)|, |g(1; \theta)|\} \\ 602 \quad &\leq \sup_{\theta \in K} \max\{|g(0; \theta)|, |g(1; \theta)|\} \\ 603 \quad &< +\infty \\ 604 \end{aligned}$$

605 where $K \subseteq \Theta$ is any compact containing the sequence $\{\theta_k, k \in \mathbb{N}\}$ (which exists because the se-
606 quence is convergent) and the last inequality follows from the fact that $\theta \mapsto \max\{|g(0; \theta)|, |g(1; \theta)|\}$
607 is continuous (it's the minimum of two continuous functions) and therefore bounded on K . \square

609 **Lemma A.4.** *Let $R \subseteq \mathbb{R}^k$ be a compact set and let the functions $f(\cdot, x) : [a, b] \rightarrow \mathbb{R}$ be continuous,
610 linear splines on a common grid $a = u_1 < \dots < u_{n+1} = b$, for every $x \in R$. Then there exists a
611 subset $\Theta \subseteq \Theta(n)$ (which depends only on the grid) such that the set-valued function $\tilde{\theta} : R \rightrightarrows \Theta$,
612 defined by*

$$614 \quad \tilde{\theta}(x_{PA(k)}) := \arg \min_{\theta' \in \Theta} \|\hat{f}(\cdot, x_{PA(k)}) - g(\cdot, \theta')\|_{L^1([0, 1])}, \quad \forall x_{PA(k)} \in R$$

616 *admits a continuous selection $\theta : R \rightarrow \Theta$, such that $g(u, \theta(x)) = \hat{f}(u, x)$ for all $u \in [0, 1]$.*

618 *Proof.* The existence of a continuous selection follows from Michael's theorem (Aubin &
619 Frankowska, 2009, Theorem 9.1.2), provided we can show that $\tilde{\theta}$ is lower semi-continuous with
620 closed and convex values.

622 Lower-semicontinuity actually holds regardless of the choice of the set Θ , so we prove it first. It
623 follows from the fact that that $(x_{PA(k)}, \theta) \mapsto \|\hat{f}(u, x_{PA(k)}) - g(u; \theta')\|_{L^1([0, 1])}$ is a Carathéodory
624 function (for a definition, see Rockafellar & Wets (1998, Example 14.29)) and therefore a normal
625 integrand (Rockafellar & Wets, 1998, Definition 14.27, Proposition 14.28). Indeed:

- 627 • Since $(u, x_{PA(k)}) \mapsto |\hat{f}(u, x_{PA(k)}) - g(u; \theta)|$ is measurable (even continuous) for all
628 $\theta \in \Theta$, Tonelli's theorem (Folland, 1999, Theorem 2.37) implies that $x \mapsto \|\hat{f}(\cdot, x) -$
629 $g(\cdot; \theta)\|_{L^1([0, 1])}$ is measurable.
- 631 • The map $\theta \mapsto h(x_{PA(k)}, \theta)$ is continuous for all $x_{PA(k)} \in \mathbb{R}^{|PA(k)|}$ because it's the com-
632 position of two continuous maps: $\theta \mapsto g(\cdot; \theta) \in L^1([0, 1])$, which is continuous by Lemma A.3,
633 and $g(\cdot; \theta) \mapsto \|\hat{f}(\cdot, x) - g(\cdot; \theta)\|_{L^1([0, 1])}$, which is continuous because the norm is a con-
634 tinuous function.

636 We will now show that $\tilde{\theta}$ is actually singleton valued (which, of course, implies that it is closed and
637 convex valued), by constructing a suitable set $\Theta \subseteq \Theta(n)$. The main strategy is to realize that the
638 weights and biases of the first layer ($w^{(1)}$ and $b^{(1)}$) can be used to fully specify the segments on
639 which the function $u \mapsto g(u, \theta)$ is piecewise linear and that, once this choice is made, the weights
640 and the bias of the second layer ($w^{(2)}$ and $b^{(2)}$) determine *uniquely* the slope and intercepts on each
641 segment.

642 More specifically, given the grid $a = u_1 < u_2 < \dots < u_{n+1} = b$, denote by

$$644 \quad \Delta u_i := u_{i+1} - u_i \text{ and } m_i := \frac{1}{2}(u_{i+1} + u_i), \quad (i = 1, \dots, n)$$

645 the width and the midpoint of each grid segment, respectively. If we set

$$647 \quad \bar{w}_i^{(1)} = 2/\Delta u_i, \quad \bar{b}_i^{(1)} = -m_i \Delta u_i, \quad (i = 1, \dots, n)$$

648 and define $\Theta := \{\bar{w}^{(1)}\} \times \{\bar{b}^{(1)}\} \times \mathbb{R}_{>0} \times \mathbb{R} \subseteq \Theta(n)$, then $g(\cdot, \theta)$ is piecewise linear exactly on the
 649 grid $\{u_i\}_{i=1}^{n+1}$, for any $\theta \in \Theta$. Additionally on each segment $[u_i, u_{i+1}]$, the function $g(\cdot, \theta)$ has slope
 650

651
$$w_i^{(2)} \left(\bar{w}_i^{(1)} + \frac{\alpha}{2} \sum_{j \neq i} \bar{w}_j^{(1)} \right)$$

 652
 653
 654

655 and bias

656
$$w_i^{(2)} \bar{b}_i^{(1)} + nb^{(2)} + (n-1) \frac{\alpha}{2} w_j^{(2)} \bar{b}_j^{(1)} + \left(\frac{\alpha}{2} - 1 \right) \left(\sum_{j < i} w_j^{(2)} - \sum_{j > i} w_j^{(2)} \right).$$

 657
 658
 659

660 We can therefore exactly match any continuous, strictly increasing, piecewise linear function on the
 661 grid $\{u_i\}_{i=1}^{n+1}$ by matching the slope and intercept on $[u_1, u_2]$, together with the slopes on each of
 662 the remaining segments (the intercepts will be automatically matched by continuity). This is a linear
 663 system of $n+1$ equations in $n+1$ unknowns and it always admits a unique solution (as can be readily
 664 checked), which implies that for every $x \in R$ we can find a $\theta \in \Theta$ such that $g(u, \theta) = \hat{f}(u, x)$ for
 665 all $u \in [a, b]$. \square
 666

667 **Lemma A.5.** *Let $g \in \text{IncrMLP}(n)$. Then $\theta \mapsto g(u, \theta)$ is locally Lipschitz uniformly in $u \in [0, 1]$,
 668 i.e. for every compact $K \subseteq \Theta(n)$ there exists an $L > 0$ such that:*

669
$$|g(u, \theta) - g(u, \hat{\theta})| \leq L \|\theta - \hat{\theta}\|, \quad \forall \theta, \hat{\theta} \in K, \forall u \in [0, 1].$$

 670
 671

672 *Proof.* The proof follows by direct computation. We use repeatedly the Cauchy-Schwartz inequality,
 673 the fact that the activation ρ is 1-Lipschitz and that $\|u\| \leq 1$:

674
$$\begin{aligned} |g(u, \theta) - g(u, \hat{\theta})| &\leq |\langle w^{(2)}, \rho^{\otimes n}(uw^{(1)} + b^{(1)}) \rangle + b^{(2)} - \langle \hat{w}^{(2)}, \rho^{\otimes n}(u\hat{w}^{(1)} + \hat{b}^{(1)}) \rangle - \hat{b}^{(2)}| \\ &\leq |\langle w^{(2)}, \rho^{\otimes n}(uw^{(1)} + b^{(1)}) \rangle - \langle \hat{w}^{(2)}, \rho^{\otimes n}(uw^{(1)} + b^{(1)}) \rangle| \\ &\quad + |\langle \hat{w}^{(2)}, \rho^{\otimes n}(uw^{(1)} + b^{(1)}) \rangle - \langle \hat{w}^{(2)}, \rho^{\otimes n}(u\hat{w}^{(1)} + \hat{b}^{(1)}) \rangle| + |b^{(2)} - \hat{b}^{(2)}| \\ &= |\langle w^{(2)} - \hat{w}^{(2)}, \rho^{\otimes n}(uw^{(1)} + b^{(1)}) \rangle| \\ &\quad + |\langle \hat{w}^{(2)}, \rho^{\otimes n}(uw^{(1)} + b^{(1)}) - \rho^{\otimes n}(u\hat{w}^{(1)} + \hat{b}^{(1)}) \rangle| + |b^{(2)} - \hat{b}^{(2)}| \\ &\leq \|w^{(2)} - \hat{w}^{(2)}\| \|\rho^{\otimes n}(uw^{(1)} + b^{(1)})\| \\ &\quad + \|\hat{w}^{(2)}\| \|\rho^{\otimes n}(uw^{(1)} + b^{(1)}) - \rho^{\otimes n}(u\hat{w}^{(1)} + \hat{b}^{(1)})\| + |b^{(2)} - \hat{b}^{(2)}| \\ &\leq \|w^{(2)} - \hat{w}^{(2)}\| (\|w^{(1)}\| + \|b^{(1)}\|) + \|\hat{w}^{(2)}\| (\|w^{(1)} - \hat{w}^{(1)}\| + \|b^{(1)} - \hat{b}^{(1)}\| + |b^{(2)} - \hat{b}^{(2)}|) \end{aligned}$$

 675
 676
 677
 678
 679
 680
 681
 682
 683
 684
 685
 686

687 Since the parameters are contained in a compact K , their norms are bounded by a constant, say
 688 $M > 0$, so that:

689
$$\begin{aligned} |g(u, \theta) - g(u, \hat{\theta})| &\leq 2M(\|w^{(2)} - \hat{w}^{(2)}\| + \|w^{(1)} - \hat{w}^{(1)}\| + \|b^{(1)} - \hat{b}^{(1)}\| + |b^{(2)} - \hat{b}^{(2)}|) \\ &\leq 2M\sqrt{4}\|\theta - \hat{\theta}\| \end{aligned}$$

 690
 691
 692

693 where the last inequality is due to Cauchy-Schwartz (this time applied to the (four-dimensional)
 694 vector of parameters' norms and the four-dimensional unit vector). \square
 695

696 **Lemma A.6.** *Let $(u, x_{PA}(k)) \mapsto F_k^{-1}(u \mid x_{PA}(k))$ be as in Theorem 4.4. Then:*

697

- 698 i) $F_k^{-1}(u \mid x_{PA}(k)) \in L^1(du \otimes \mu(dx_{PA}(k)))$,
- 699 ii) $\partial_u F_k^{-1}(u \mid x_{PA}(k)) \in L^1(du \otimes \mu(dx_{PA}(k)))$,
- 700 iii) $\partial_{x_j} F_k^{-1}(u \mid x_{PA}(k)) \in L^1(du \otimes \mu(dx_{PA}(k)))$, for all $j \in PA(k)$.

702 *Proof.* i) By direct integration:

$$\begin{aligned}
 & \int_{\mathbb{R}^{|\text{PA}(k)|}} \mu(dx_{\text{PA}(k)}) \int_{[0,1]} du |F_k^{-1}(u \mid x_{\text{PA}(k)})| \\
 &= \int_{\mathbb{R}^{|\text{PA}(k)|}} \mu(dx_{\text{PA}(k)}) \int_{\mathbb{R}} \mu(dx_k \mid x_{\text{PA}(k)}) |x_k| \\
 &= \int_{\mathbb{R}} \mu(dx_k) |x_k| \leq +\infty
 \end{aligned}$$

711 where we have first used the change-of-variable formula (Bogachev, 2007, Theorem 3.6.1) with
712 $F_k^{-1}(\cdot \mid x_{\text{PA}(k)}) \# \mathcal{U}[0,1] = \mu(dx_k \mid x_{\text{PA}(k)})$ (McNeil et al., 2015, Proposition A.6) and then used
713 the fact that μ has finite first moments.

715 ii) $u \mapsto F^{-1}(u \mid x)$ is increasing on the closed interval $[0, 1]$, therefore by Bogachev (2007, Corol-
716 lary 5.2.7) it is almost everywhere differentiable and:

$$\int_{[0,1]} |\partial_u F_k^{-1}(u \mid x_{\text{PA}(k)})| du \leq F_k^{-1}(1 \mid x_{\text{PA}(k)}) - F_k^{-1}(0 \mid x_{\text{PA}(k)}).$$

721 The right-hand side is just $\text{diam}(\text{supp}(\mu(dx_k \mid x_{\text{PA}(k)})))$, which is finite, since μ is compactly
722 supported.

723 iii) Continuity of $u \mapsto F_k(u \mid x_{\text{PA}(k)})$ implies that $F_k(F_k^{-1}(u \mid x_{\text{PA}(k)})) = u$ (McNeil et al., 2015,
724 Proposition A.3 (viii)). Differentiating this expression on both sides and using the chain rule
725 yields:

$$\begin{aligned}
 \int_{[0,1]} |\partial_{x_j} F_k^{-1}(u \mid x_{\text{PA}(k)})| du &= \int_{[0,1]} du \left| -\frac{\partial_{x_j} F_k(F_k^{-1}(u \mid x_{\text{PA}(k)}) \mid x_{\text{PA}(k)})}{\partial_u F_k(F_k^{-1}(u \mid x_{\text{PA}(k)}) \mid x_{\text{PA}(k)})} \right| \\
 &= \int_{\mathbb{R}} dx' \left| -\partial_{x_j} F_k(x' \mid x_{\text{PA}(k)}) \right|,
 \end{aligned}$$

732 where the second equality follows from the same change-of-variable as in part (i) and by sim-
733 plifying the conditional density. The claim now follows by integrating over $\mathbb{R}^{|\text{PA}(k)|}$ with respect
734 to $\mu(dx_{\text{PA}(k)})$ and using the assumption that $(x_k, x_{\text{PA}(k)}) \mapsto F_k(x_k \mid x_{\text{PA}(k)})$ is a C^1 map and
735 therefore admits bounded partial derivatives on compacts.

□

B PROOFS

B.1 PROOF OF THEOREM 3.7

743 *Proof.* We generalize the proof by Acciaio et al. (2024) to our G -causal setting. Given $\mu, \nu \in$
744 $\mathcal{P}_G(\mathbb{R}^d)$, let g be a G -causal function and let π be the optimal G -bicausal coupling between μ and
745 ν . Then:

$$\begin{aligned}
 -\mathbb{E}^\nu [Q(X_T, g(X_{V \setminus T}))] &= - \int Q(x'_T, g(x'_{V \setminus T})) \nu(dx') \\
 &= - \int Q(x'_T, g(x'_{V \setminus T})) \pi(dx, dx') \\
 &= \int (Q(x_T, g(x'_{V \setminus T})) - Q(x'_T, g(x'_{V \setminus T}))) \pi(dx, dx') - \int Q(x_T, g(x'_{V \setminus T})) \pi(dx, dx')
 \end{aligned}$$

754 Since $x \mapsto Q(x, g)$ is uniformly locally L -Lipschitz, the first integral satisfies:

$$\begin{aligned}
& \int \left(Q(x_T, g(x'_{V \setminus T})) - Q(x'_T, g(x'_{V \setminus T})) \right) \pi(dx, dx') \leq L \int \|x_T - x'_T\| \pi(dx, dx') \\
& \leq L \int \|x - x'\| \pi(dx, dx') \\
& = L \cdot W_G(\mu, \nu)
\end{aligned}$$

For the second integral, we notice that:

$$\begin{aligned}
& - \int Q(x_T, g(x'_{V \setminus T})) \pi(dx, dx') \leq - \int Q \left(x_T, \int g(x'_{V \setminus T}) \pi(dx' | x) \right) \mu(dx) \\
& = - \int Q \left(x_T, \underbrace{\int g(x'_{\text{PA}(T)}) \pi(dx' | x)}_{h(x)} \right) \mu(dx)
\end{aligned}$$

where we first applied Jensen's inequality and then the fact that g is G -causal. Furthermore, since π is G -causal, the function $h(x) := \int g(x'_{V \setminus T}) \pi(dx' | x)$ actually depends only on $x_{\text{PA}(T) \cup \text{PA}(\text{PA}(T))}$. To ease the notation, denote $A := \text{PA}(T) \cup \text{PA}(\text{PA}(T))$. Then:

$$\begin{aligned}
& - \int Q(x_T, h(x_A)) \mu(dx) = - \int \mu(dx_A) \int \mu(dx_T | x_A) Q(x_T, h(x_A)) \\
& = - \int \mu(dx_A) \int \mu(dx_T | x_{\text{PA}(T)}) Q(x_T, h(x_A)) \\
& \leq - \int \mu(dx_A) \int \mu(dx_T | x_{\text{PA}(T)}) Q(x_T, h^*(x_{\text{PA}(T)})) \\
& = - \mathcal{V}(\mu)
\end{aligned}$$

where in the second equality we have used the fact that $X_T \perp\!\!\!\perp X_A | X_{\text{PA}(T)}$ (see condition (ii) in Definition 2.2 or simply notice that $X_{\text{PA}(T)}$ d -separates X_T and $X_{\text{PA}(\text{PA}(T))}$), while the inequality is due to Eq. (1).

Putting everything together:

$$-\mathbb{E}^\nu [Q(Y, g(X))] \leq L \cdot W_G(\mu, \nu) - \mathcal{V}(\mu)$$

and, since g is arbitrary, we obtain:

$$\mathcal{V}(\mu) - \mathcal{V}(\nu) \leq L \cdot W_G(\mu, \nu).$$

By symmetry, exchanging μ and ν yields the same inequality for the term $\mathcal{V}(\nu) - \mathcal{V}(\mu)$, therefore

$$|\mathcal{V}(\mu) - \mathcal{V}(\nu)| \leq L \cdot W_G(\mu, \nu).$$

□

B.2 PROOF OF THEOREM 4.4

Proof. We know that $\mu = T_\# \mathcal{N}(0, I_d)$, where $T = T^{(d)} \circ \dots \circ T^{(1)}$ is the G -compatible, increasing transformation in the statement of Theorem 4.3. Now, let $\hat{T} = \hat{T}^{(d)} \circ \dots \circ \hat{T}^{(1)} \in G\text{-NF}(d)$ be a G -NF with flows as in Eq. (2) and define the G -bicausal coupling $\pi := (T, \hat{T})_\# \mathcal{N}(0, 1)$, then we have that:

$$W_G(\mu, \hat{T}_\# \lambda) \leq \int_{\mathbb{R}^d \times \mathbb{R}^d} \|x - x'\| \pi(dx, dx') = \int_{[0,1]^d} \|T(u) - \hat{T}(u)\| du.$$

We can make the right-hand side smaller than any $\varepsilon > 0$ by using Lemma A.2 (with $\mathcal{X} := [0, 1]^d$, $\mu^{(0)} := \mathcal{U}([0, 1]^d)$ and $\mu^{(k)} := \mu_{1:k} \otimes \mathcal{U}([0, 1]^{d-k})$, for $k = 1, \dots, d$), provided that we can show that conditions (i) and (ii) therein hold.

810 **Condition (i).** Each hypercoupling flow $\hat{T}^{(k)}$ differs from the identity only at its k -th coordinate,
 811 which is the output of a shallow MLP (see Eq. (2)). But shallow MLPs are Lipschitz functions of
 812 their input, therefore each $\hat{T}^{(k)}$ is a Lipschitz function.
 813

814 **Condition (ii).** We need to show that for every $\varepsilon > 0$, there exists an $n \in \mathbb{N}$, a $\hat{\theta}(\cdot) \in \text{MLP}$ and a
 815 $g(\cdot, \hat{\theta}(x_{\text{PA}(k)})) \in \text{IncrMLP}(n)$ such that

$$816 \quad \int_{[0,1]} du \int_{\mathbb{R}^{|\text{PA}(k)|}} \mu(dx_{\text{PA}(k)}) |F_k^{-1}(u | x_{\text{PA}(k)}) - g(u; \hat{\theta}(x_{\text{PA}(k)}))| \leq \varepsilon. \quad (7)$$

819 We will prove this bound by splitting the error into three terms and bounding each one separately.

820 **Term 1.** First we approximate $(u, x_{\text{PA}(k)}) \mapsto F_k^{-1}(u | x_{\text{PA}(k)})$ with a continuous tensor-product
 821 linear spline, $\hat{f}(u, x_{\text{PA}(k)})$, on the rectangle $[0, 1] \times R$, where $R = \prod_{j=1}^{|\text{PA}(k)|} [a_j, b_j]$ is a rectangle
 822 large enough to contain the compact support of $\mu(dx_{\text{PA}(k)})$. We choose the approximation grid fine
 823 enough to satisfy:

$$825 \quad \int_{[0,1]} du \int_{\mathbb{R}^{|\text{PA}(k)|}} \mu(dx_{\text{PA}(k)}) |F_k^{-1}(u | x_{\text{PA}(k)}) - \hat{f}(u, x_{\text{PA}(k)})| \leq \varepsilon/2,$$

827 and let $n + 1$ be the number of gridpoints in the u -axis (i.e. the grid on $[0, 1]$ has gridpoints $0 =$
 828 $u_1 < \dots < u_{n+1} = 1$).

830 The validity of this approximation follows from (Schumaker, 2007, Theorem 12.7) and requires that
 831 $(u, x) \mapsto F^{-1}(u | x)$ belong to a suitable tensor Sobolev space (Schumaker, 2007, Example 13.5), as
 832 we verify in Lemma A.6.

833 **Term 2.** Next, we approximate the univariate functions $u \mapsto \hat{f}(u, x_{\text{PA}(k)})$, for each $x_{\text{PA}(k)} \in R$, with
 834 neural networks $g(\cdot; \theta(x_{\text{PA}(k)})) \in \text{IncrMLP}(n)$, by judiciously choosing the function $\theta : R \rightarrow \Theta(n)$.
 835

836 Since all the functions $\hat{f}(\cdot, x_{\text{PA}(k)})$ share the same grid on $[0, 1]$, by Lemma A.4 there exists a param-
 837 eter subset $\Theta \subseteq \Theta(n)$ (which depends only on this grid) such that the set-valued map $\tilde{\theta} : R \rightrightarrows \Theta$,
 838 defined as

$$839 \quad \tilde{\theta}(x_{\text{PA}(k)}) := \arg \min_{\theta' \in \Theta} \|\hat{f}(\cdot, x_{\text{PA}(k)}) - g(\cdot, \theta')\|_{L^1([0,1])},$$

840 admits a continuous selection $\theta : R \rightarrow \Theta$. We then use this function θ to parametrize the neural
 841 networks $g(\cdot, \theta(x_{\text{PA}(k)}))$ and, as implied by Lemma A.4, this parametrization is optimal, in the sense
 842 that $g(u, \theta(x_{\text{PA}(k)})) = \hat{f}(u, x_{\text{PA}(k)})$ for all $u \in [0, 1]$, thus achieving zero approximation zero, i.e.
 843

$$844 \quad \int_{[0,1]} du \int_{\mathbb{R}^{|\text{PA}(k)|}} \mu(dx_{\text{PA}(k)}) |\hat{f}(u, x_{\text{PA}(k)}) - g(u, \theta(x_{\text{PA}(k)}))| = 0.$$

848 **Term 3.** Finally, we approximate $g(u; \theta(x_{\text{PA}(k)}))$ with $g(u; \hat{\theta}(x_{\text{PA}(k)}))$, where $\hat{\theta}(\cdot)$ is a suitable MLP.

849 Since $\theta : R \rightarrow \Theta$ is a continuous function on a compact, we have that $\theta \in L^1(\mu)$, therefore for
 850 every $\varepsilon' > 0$ there is an MLP⁷ $\hat{\theta}$ such that $\|\theta - \hat{\theta}\|_{L^1(\mu)} \leq \varepsilon'$ (Leshno et al., 1993, Proposition 1).

852 Therefore:

$$853 \quad \int_{[0,1]} du \int_{\mathbb{R}^{|\text{PA}(k)|}} \mu(dx_{\text{PA}(k)}) |g(u; \theta(x_{\text{PA}(k)})) - g(u; \hat{\theta}(x_{\text{PA}(k)}))| \\ 854 \quad \leq \int_{[0,1]} du \int_{\mathbb{R}^{|\text{PA}(k)|}} \mu(dx_{\text{PA}(k)}) L \|\theta(x_{\text{PA}(k)}) - \hat{\theta}(x_{\text{PA}(k)})\| \\ 855 \quad \leq L\varepsilon' \leq \varepsilon/2 \quad (\text{choose } \varepsilon' = \varepsilon/2L)$$

859 where the first inequality follows from the uniform local Lipschitz property on the compact
 860 $\theta(\text{supp}(\mu)) \cup \hat{\theta}(\text{supp}(\mu))$ proved in Lemma A.5.

862 Summing all three approximation errors together, we obtain the bound in Eq. (7). \square

863 ⁷For the theorem to hold we only need the activation function to be non-polynomial and locally essentially
 bounded (such as ReLU).

864 B.3 PROOF OF THEOREM 4.6
865866 *Proof.* First we notice that

867
$$W_G(\mu, \nu) = \min_{\pi \in \Pi_G^{bc}(\mu, \nu)} \int_{\mathbb{R}^d \times \mathbb{R}^d} \|x - x'\| \pi(dx, dx')$$

868
$$\leq \min_{\pi \in \Pi_G^{bc}(\mu, \nu)} \int_{\mathbb{R}^d \times \mathbb{R}^d} \text{diam}(K) \cdot \mathbf{1}_{\{x \neq x'\}}, \pi(dx, dx')$$

869
$$=: \text{diam}(K) \cdot d_{G-TV}(\mu, \nu)$$

870 where in the last equality we have introduced the G -causal total variation distance, $d_{G-TV}(\cdot, \cdot)$, as a
871 suitable generalization of the total variation distance for G -bicausal couplings.
872873 The claim then follows by showing that $d_{G-TV}(\mu, \nu) \leq (2^d - 1)d_{TV}(\mu, \nu)$ for all sorted DAGs G by
874 induction on the number of vertices, which is a straightforward but tedious generalization of Eckstein
875 & Pammer (2024, Lemma 3.5) to our G -causal setting.
876877 The claim holds trivially if G has only one vertex (all couplings are G -bicausal). Suppose now the
878 claim is true for all sorted DAGs on n vertices. Then for a sorted DAG G on $n + 1$ vertices, denote
879 by G_n its subgraph on vertices $\{1, \dots, n\}$. We start with some definitions. Define:
880

881
$$\eta(dx_{n+1}|x_{PA(n+1)}) := \mu(dx_{n+1}|x_{PA(n+1)}) \wedge \nu(dx_{n+1}|x_{PA(n+1)}),$$

882
$$\pi \in \Pi_G^{bc}(\mu, \nu) \text{ as } \pi := \pi_n \otimes \pi(dx_{n+1}, dx'_{n+1} | x_{PA(n+1)}, x'_{PA(n+1)}),$$

883 where $\pi_n \in \Pi_{G_n}^{bc}(\mu(dx_{1:n}), \nu(dx'_{1:n}))$, and:
884

885
$$\pi(dx_{n+1}, dx'_{n+1} | x_{PA(n+1)}, x'_{PA(n+1)}) := \begin{cases} \sigma(dx_{n+1}, dx'_{n+1} | x_{PA(n+1)}, x'_{PA(n+1)}) & \text{if } x_{PA(n+1)} = x'_{PA(n+1)} \\ \mu(dx_{n+1} | x_{PA(n+1)}) \otimes \nu(dx'_{n+1} | x'_{PA(n+1)}) & \text{otherwise} \end{cases}$$

886 where σ is the optimal coupling for the (conditional) total variation distance, i.e.:
887

888
$$\sigma(dx_{n+1}, dx'_{n+1} | x_{PA(n+1)}, x'_{PA(n+1)}) := (\text{id}, \text{id})_{\#} \eta(dx_{n+1}|x_{PA(n+1)}) + (\mu(dx_{n+1}|x_{PA(n+1)}) - \eta(dx_{n+1}|x_{PA(n+1)})) \otimes (\nu(dx_{n+1}|x_{PA(n+1)}) - \eta(dx_{n+1}|x_{PA(n+1)}))$$

889 Then the following bounds can be established (see Eckstein & Pammer (2024, Lemma 3.5) for
890 step-by-step details):
891

892
$$d_{G-TV}(\mu, \nu) \leq \int \mathbf{1}_{\{x \neq x'\}} \pi(dx, dx')$$

893
$$= \int \mathbf{1}_{\{x_{1:n} \neq x'_{1:n}\}} \pi_n(dx_{1:n}, dx'_{1:n})$$

894
$$+ \int d_{TV}(\mu(dx_{n+1}|x_{PA(n+1)}), \nu(dx_{n+1}|x_{PA(n+1)})) \mathbf{1}_{\{x_{1:n} = x'_{1:n}\}} \pi_n(dx_{1:n}, dx'_{1:n})$$

895
$$= \int \mathbf{1}_{\{x_{1:n} \neq x'_{1:n}\}} \pi_n(dx_{1:n}, dx'_{1:n}) + \|\eta \otimes (\mu(dx_{n+1}|x_{PA(n+1)}) - \nu(dx_{n+1}|x_{PA(n+1)}))\|_{TV}$$

896 For all $A \in \mathbb{R}^{n+1}$, one has:
897

898
$$\eta \otimes (\mu(dx_{n+1}|x_{PA(n+1)}) - \nu(dx_{n+1}|x_{PA(n+1)}))(A) \leq \|\mu(dx_{n+1}|x_{PA(n+1)}) - \nu(dx_{n+1}|x_{PA(n+1)})\|_{TV}$$

899
$$+ \int \mathbf{1}_{\{x_{1:n} \neq x'_{1:n}\}} \pi_n(dx_{1:n}, dx'_{1:n})$$

900 Putting the two bounds together and minimizing over all G_n -bicausal couplings π_n :
901

902
$$d_{G-TV}(\mu, \nu) \leq 2d_{G_n-TV}(\mu_{1:n}, \nu_{1:n}) + d_{TV}(\mu, \nu)$$

903
$$\leq (2^{n+1} - 2 + 1)d_{TV}(\mu, \nu)$$

904
$$= (2^{n+1} - 1)d_{TV}(\mu, \nu)$$

905 where we have used:
906

907
$$d_{G_n-TV}(\mu_{1:n}, \nu_{1:n}) \leq (2^n - 1)d_{TV}(\mu_{1:n}, \nu_{1:n}) \leq (2^n - 1)d_{TV}(\mu, \nu),$$

908 which follows from the induction hypothesis and the data pre-processing inequality for the total
909 variation distance (Eckstein & Nutz, 2022, Lemma 4.1). \square
910